Since January 2020 Elsevier has created a COVID-19 resource centre with free information in English and Mandarin on the novel coronavirus COVID-19. The COVID-19 resource centre is hosted on Elsevier Connect, the company's public news and information website.

Computers in Biology and Medicine 139 (2021) 104965

Contents lists available at ScienceDirect

Computers in Biology and Medicine

journal homepage: www.elsevier.com/locate/compbiomed

Potential of turmeric-derived compounds against RNA-dependent RNA polymerase of SARS-CoV-2: An *in-silico* approach

Rahul Singh [a,b,1], Vijay Kumar Bhardwaj [a,b,c,1], Rituraj Purohit [a,b,c,*]

[a] Structural Bioinformatics Lab, CSIR-Institute of Himalayan Bioresource Technology (CSIR-IHBT), Palampur, HP, 176061, India
[b] Biotechnology Division, CSIR-IHBT, Palampur, HP, 176061, India
[c] Academy of Scientific & Innovative Research (AcSIR), Ghaziabad-201002, India

ARTICLE INFO

Keywords:
COVID-19
RdRp-RNA
SARS-CoV-2
Curcumin
Diacetylcurcumin
MM-PBSA

ABSTRACT

The Severe Acute Respiratory Syndrome Coronavirus 2 (SARS-CoV-2) is the causative agent of the COVID-19 pandemic. Currently, there are no particular antivirals available to battle with COVID-19. The RNA-dependent RNA polymerase (RdRp) has emerged as a novel drug target due to its essential role in virus replication. In this study, turmeric-derived compounds were chosen and subjected to *in-silico* analysis to evaluate their binding affinity against the RdRp-RNA complex of SARS-CoV-2. Our *in-silico* approach included the analysis of protein-ligand interactions by molecular docking and molecular dynamics simulations, followed by free energy calculations by molecular mechanics Poisson-Boltzmann surface area analysis. Curcumin and diacetylcurcumin showed stability and good binding affinity at the active site of the SARS-CoV-2 RdRp-RNA complex. Furthermore, to validate the potency of selected compounds, we compared them with Favipiravir and Remdesivir antiviral drugs from our previous analysis on targeting tea bioactive molecules to inhibit RdRp-RNA complex. The comparative analysis revealed that the selected compounds showed higher potential to be developed as RdRp-RNA inhibitors than antiviral medicines Remdesivir and Favipiravir. However, these compounds need to be further validated by *in-vitro* and *in-vivo* investigations.

1. Introduction

The newly emerged coronavirus (CoV) known as the Severe Acute Respiratory Syndrome Coronavirus 2 (SARS-CoV-2) is the causative agent of the COVID-19 disease. Correlated to the other CoVs, the transmission frequency of SARS-CoV-2 (between human beings) is higher, which describes its widespread [1,2]. The non-structural protein 12 (Nsp12) of SARS-CoV-2, also known as the RNA-dependent RNA polymerase (RdRp) is one of the most crucial targets for viral inhibition because it catalyzes the synthesis of viral RNA during transcription and replication of SARS-CoV-2 [3,4]. The RdRp is aided by cofactors such as Nsp7 and Nsp8 [5]. The RdRp structure consists of a polymerase domain (residues Ser367 to Phe920) and a nidovirus-specific N-terminal expansion domain (NiRAN domain) composed of residues from Asp60 to Arg249 [6,7]. Both these domains are joined by the interface domain (residues Ala250 to Arg365) [4]. The RdRp includes three other domains, the palm domain (Tyr582-Pro620 and Tyr680-Gln815), fingers domain (Leu366-Ala581 and Lys621-Gly679), and the thumb domain (His816-Glu920). The overall stability of the structure is aided by an N-terminal hairpin (residues Asp29 to Lys50) structure located between the NiRAN domain and the palm subdomain [4,6]. The structure consists of five antiparallel β-strands and two helices present between residues Ala4 and Arg118 [4,8]. Also, an additional β-strand present between residues Asn215 and Asp218 combines with another strand (residue Val96 to Ala100) to render conformational stability by building a compact and stable-barrel structure [4].

The RdRp participates in the RNA synthesis (template-directed) part of the life cycle of the SARS-CoV-2. The template insertion, nucleoside triphosphate (NTP) entry, and developing strand exit pathway merge inside a positively charged middle cavity [4,9]. The hydrophilic motif F defines the NTP entry channel (residues Lys545, Arg553, and Arg555) [4]. The template RNA enters the binding site via motifs F and G, with the template strand held by motif E and the thumb subdomain. The binding site contains motifs A and C, supported by motifs B and D [8]. The global SARS-CoV-2 spread and increasing statistics highlight the significance of identifying therapeutic candidates that could effectively

* Corresponding author. Structural Bioinformatics Lab, CSIR-Institute of Himalayan Bioresource Technology (CSIR-IHBT), Palampur, HP, 176061, India.
E-mail addresses: rituraj@ihbt.res.in, riturajpurohit@gmail.com (R. Purohit).
[1] Equal Contribution.

https://doi.org/10.1016/j.compbiomed.2021.104965
Received 11 August 2021; Received in revised form 18 October 2021; Accepted 18 October 2021
Available online 22 October 2021

manage the spreading pandemic. The RdRp is an assuring target for inhibition for several reasons: first, it plays an indispensable role in the life cycle of the virus; second, the character of protein structure and conserved sequences across different RNA viruses; finally, there are no homologous proteins present in the host system [4,10]. Remdesivir is a nucleotide analog (NA) that has proven to be efficient against various virus-related infections and has been proclaimed to halt the proliferation of SARS-CoV-2 [11,12]. When NAs enter the cell, they produce an active 5 -triphosphate, which competes with endogenic nucleotides for incorporation into RNA (viral) by serving as a substitute for RdRp substrate [3].

Natural molecules consist of high chemical variety, lower production price, and fewer side effects than molecules synthesized from combinatorial/synthetic chemistry. Hence, an effort was made to screen and evaluate the potential of turmeric-derived molecules against the RdRp of SARS-CoV-2 using computational tools. Turmeric (*Curcuma longa*) is a spice utilized in daily food uptake and also used as an anti-inflammatory agent in Ayurveda remedies. It was also reported that curcumin inhibits viral infection by intervening with various replication events [13]. Curcumin was also reported to interfere in binding of Chikungunya and Zika virus cells with the cell membrane of host cells [14]. In this study, we prepared a library of turmeric-derived molecules, and all the molecules docked inside the binding site of RdRp-RNA. Further, these molecules were analyzed by various structural parameters of molecular dynamics (MD) simulation analyses. Our results provide a basis for further experimental and clinical investigations of the suggested lead molecules.

2. Material and methods

2.1. Datasets

The crystal structure of RdRp from the Protein data bank (PDB ID: 7BV2) with 2.5 Å resolution was retrieved [4]. The protein structure includes Nsp12 (RdRp) associated with cofactors Nsp7, Nsp8, and primer-template RNA. We used the Pubchem database to acquire the six turmeric-derived compounds [15,16]. Compounds were prepared for molecular docking study by optimizing the ligand geometry of each compound through Gaussian16 DFT minimization protocols [17]. We adopted the "prepare protein" function of Discovery studio client 2018 to prepare missing loops of the protein [18].

2.2. Molecular docking

A set of six turmeric-derived compounds was docked with the SARS-CoV-2 RdRp-RNA. We implemented the CDOCKER; a CHARMm supported semi-flexible docking tool of the discovery studio client for molecular docking [19]. The parameters of CDOCKER were sustained default. A 10.0 Å radius, allotted from the center of the compound in the binding site, includes all the amino acids involved in binding the compound to the SARS-CoV-2 RdRp-RNA. The most reliable docking pose of each molecule accepted on the basis of the lowest interaction energy score and further appraised using Discovery studio visualizer to examine the molecular interactions.

2.3. MD simulations

Molecular dynamics (MD) simulations, conducted to elucidate further dynamic actions of the Curcumin and diacetylcurcumin inside the binding site of RdRp-RNA and confirm the concerned binding styles from docking results. GROMACS was used to evaluate the best-docked poses by employing GROMOS96 43a1 forcefield [20]. PRODRG server used to produce ligand topologies. Simulations were carried out in a water box using a water model and neutralized the system with counter-ions. The steepest descent (energy minimization) algorithm was applied to avoid wrong associations from the original structures, and they have then subjected to NPT and NVT equilibration. We performed the NVT ensemble with a V-rescale thermostat at 300 K for 1 ns and the NPT ensemble at 1 bar pressure with Parrinello-Rahman barostat for 1 ns [21]. The geometry of the water molecules and bond constraints monitored using SETTLE and LINCS algorithms [22]. Particle Mesh Ewald (PME) was adopted to estimate long-range electrostatic and short-range non-bonded interactions [23]. We streamed MD simulations on the equilibrated NPT ensembles of every system. We used the Molecular Mechanics Poisson-Boltzmann Surface Area (MM-PBSA) procedure for every system and estimated the outcomes based on protein-ligand total energy [24].

Table 1
The docking scores in terms of -CDOCKER interaction energy (kcal/mol) for the selected turmeric-derived compounds.

S. No.	Molecules	-CDOCKER interaction energy (kcal/mol)
1.	Diacetylcurcumin	69.54
2.	Curcumin	64.10
3.	Tetrahydrocurcumin	62.1
4.	Dimethylcurcumin	58.99
5.	Demethoxycurcumin	52.95
6.	Bis-demethoxycurcumin	51.15

3. Results and discussion

At present, there are no FDA-approved antiviral medications available to treat COVID-19 patients. Emerging data suggested that turmeric-derived compounds have antiviral activity and could be used as preventive therapeutics against COVID-19 [25–28]. Turmeric possesses beneficial features such as analgesic, anti-inflammatory, antiviral, and antimicrobial activities, and hence is extensively used in Ayurveda and Siddha medical systems. The turmeric-derived compounds were computationally screened to evaluate their binding affinity with the RdRp of SARS-CoV-2.

3.1. Binding mode and intermolecular interactions

In the current study, molecular docking was adopted to predict the binding between six turmeric-derived compounds and SARS-CoV-2 RdRp-RNA protein. Molecular docking is the most widely used technique in computational drug design and discovery. The interaction energies of the six selected compounds with the SARS-CoV-2 RdRp-RNA protein were shown in Table 1. The compounds diacetylcurcumin (69.54 kcal/mol) and curcumin (64.10 kcal/mol) were selected on the basis of the best interaction energies for further analysis. The binding modes of the RdRp-RNA with two selected compounds were displayed in Fig. 1. The analysis of binding mode and intermolecular interaction showed that the bioactive molecule curcumin binds to the binding pocket by associating with the active site residues and RNA nucleotides of the template and primer strand. Curcumin interacted with uracil present at position 20 of the primer strand by alkyl interactions, two carbon-hydrogen, and two hydrogen bonds. It also formed two hydrogen bonds and two alkyl interactions with uracil at position ten of the template RNA strand. Also, curcumin interacted with adenine at position eleven of the template RNA strand by forming a carbon-hydrogen bond. Additionally, curcumin stabilized in the active site by showing hydrogen/carbon-hydrogen bonds and alkyl interactions with residues Lys545, Arg553, Ser759, Ser682, Arg555, Ala688, and Val557 of RdRp active site. Similarly, the compound diacetylcurcumin showed hydrogen bonds with residues Thr680, Asn691, Thr687, Lys545, and carbon-hydrogen bond with residue Arg555. Moreover, the residues Asp623, Val557, and Asp761 showed van der Waals interactions. Diacetylcurcumin also interacted with the primer and template RNA strands by carbon-hydrogen bonds, π-π stacked, and π-anion interactions. The residues Asp623, Ser682, and Asn691 allows selective RNA replication by identifying the RNA-specific (2′-OH) group [29]. Both the molecules

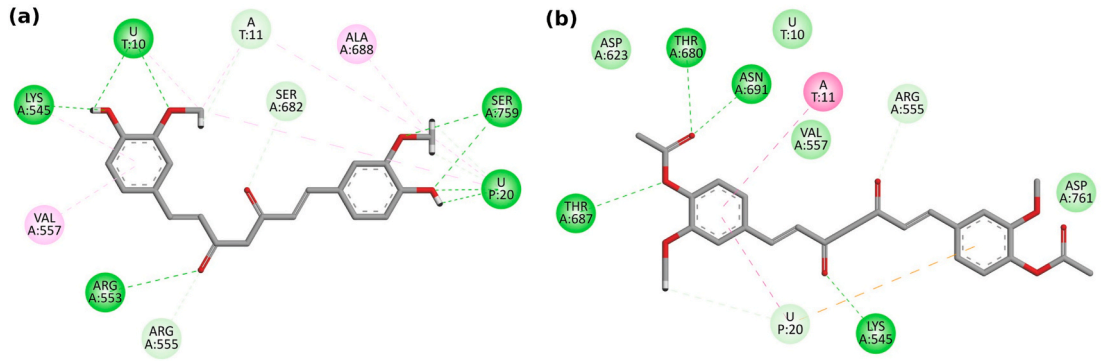

Fig. 1. The 2D interaction poses of (a) curcumin and (b) diacetylcurcumin docked on the active site of RdRp-RNA complex of SARS-CoV-2.

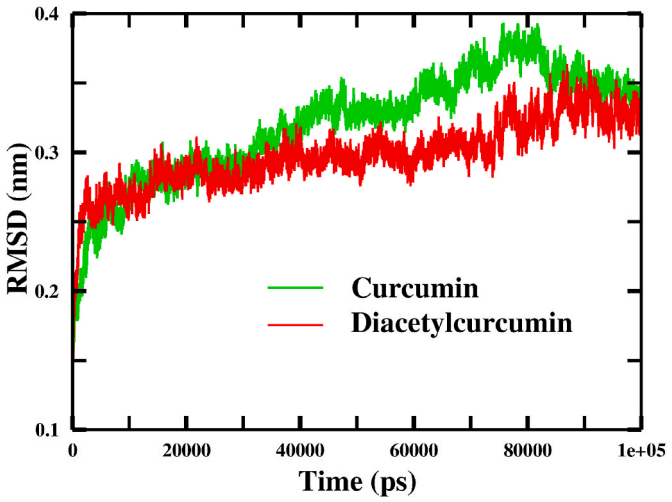

Fig. 2. Backbone RMSDs are shown as a function of time for the RdRp-RNA of SARS-CoV-2 and compounds.

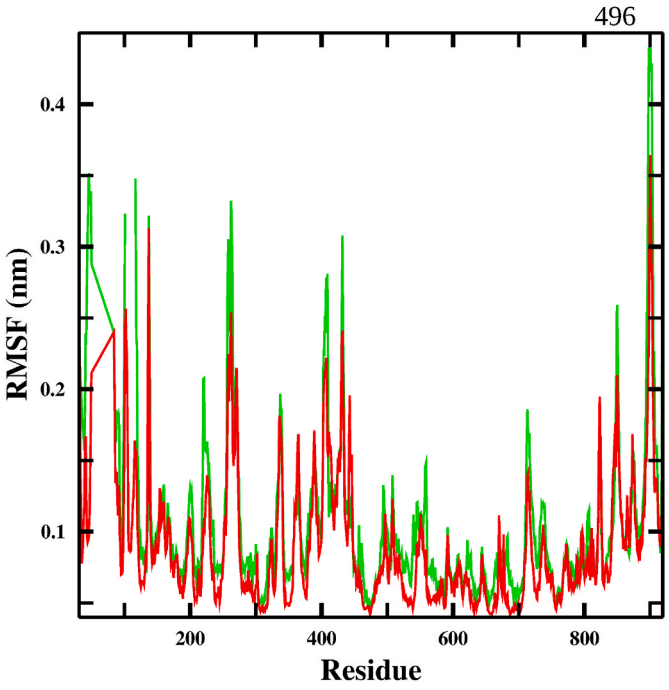

Fig. 3. RMSF for the backbone C-α-atoms of RdRp-RNA complexes with curcumin (green) and diacetylcurcumin (red).

interacted with residues Asp759, Ser761, and Asp760 which belong to the catalytic core of RdRp protein [4,30]. The residues Arg553, Lys545, and Arg555 are involved in the formation of the NTP entry channel [4], and both the selected compounds exhibited robust hydrogen bonds with these residues. We observed interactions of both the selected molecules with the RNA identifying residues and the residues forming the NTP entry channel and the catalytic core of RdRp protein. These interactions could hinder the biological activity of RdRp protein and consequently stop/interrupt the viral replication process [31]. Next, we conducted MD simulations to verify the docking poses and examine the dynamics of RdRp-RNA-ligand interactions at the catalytic pocket.

3.2. Structural stability of protein-ligand complexes

Protein-ligand interactions generated by docking are fixed poses. However, in actual biological conditions, the binding modes change depending on physiological conditions and time. The selected protein-ligand complexes were subjected to MD simulations to concede the accurate dynamic status and assessment of various bonds formed between protein and ligand [32,33]. The structural stability of the two selected RdRp-RNA-ligand complexes was analyzed by the Root mean square deviation (RMSD) analysis of backbone C-α-atoms (Fig. 2). RMSD calculations can examine the conformational variances and the structural stability of a protein-ligand complex at a global scale [34,35]. RMSD interpretation of the RdRp-RNA in complex with curcumin and diacetylcurcumin showed that both the complexes gained stability at ~100 ns. Throughout the whole simulation, both the complexes owned an average RMSD value between 0.2 and 0.4 nm. RMSD outcomes confirmed that the trajectories of both the complexes were well-equilibrated and stable.

Additionally, we analyzed the Root Mean Square Fluctuation (RMSF) values of each backbone atom in the RdRp-RNA-ligand complexes to explore the flexibility of the protein structure (Fig. 3). The higher RMSF value denotes flexibility, whereas the low RMSF value expressed limited drifts. After the equilibration of simulation, the associated complexes showed less fluctuation with a stable symmetry. It provided a framework to analyze the changes in every subset of the complexes related to the simulated structure. Both the complexes attained a smaller fluctuation in the binding site. The average fluctuations (0–0.17 nm) of both the complexes were moderate and similar to each other. RMSF analysis for the binding site area of both complexes disclosed that the residues involved in the binding of compounds were stable during the simulations.

3.3. Interaction stability analysis at different time intervals

Furthermore, it was compelling to investigate the protein-ligand poses at different time periods during the whole simulations. We obtained the scripts of selected complexes at different time periods (5 ns,

Table 2
Binding free energy in individual terms for both compounds bound to RdRp-RNA generated by MM-PBSA method.

S. No.	RdRp-RNA-Ligand Complexes	ΔE $_{binding\ (kJ/mol)}$	ΔE $_{polar\ solvation\ (kJ/mol)}$	SASA $_{(kJ/mol)}$	ΔE $_{Electrostatic\ (kJ/mol)}$	ΔE $_{Van\ der\ Waals\ (kJ/mol)}$
1.	RdRp-curcumin	−42.162	101.798	−13.496	−18.137	−112.327
2.	RdRp-diacetylcurcumin	−71.964	116.315	−19.107	−14.698	−154.474
3.	RNA-curcumin	−40.306	27.351	−6.539	−11.487	−49.631
4.	RNA-diacetylcurcumin	−80.718	31.556	−8.498	−31.535	−72.242

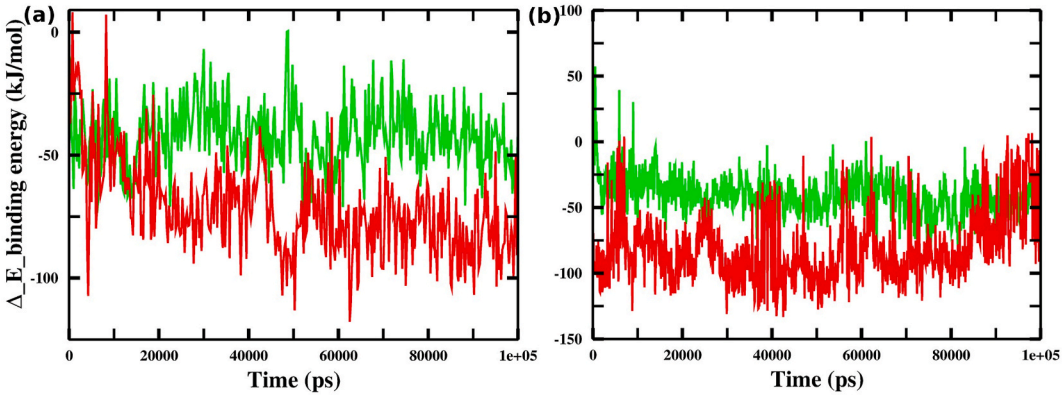

Fig. 4. The graphical representation of binding free energy estimated for the entire simulation for curcumin (green) and diacetylcurcumin (red) with (a) RdRp protein and (b) RNA respectively.

25 ns, 50 ns, 75 ns, and 100 ns) to observe the stability of the interactions in RdRp-RNA-ligand complexes (Fig. S1). The protein-ligand poses at distinct time periods reported that the interactions displayed in docking sustained during the whole simulation run. The MD simulations implied that the binding site residues manifested stable interaction poses and the selected compounds persisted in the active pocket until the simulation concludes.

3.4. Binding free energy analysis

We calculated the binding free energy based on MD simulations using the MM-PBSA procedure to determine the potency of interaction between selected compounds and RdRp-RNA complex. The higher binding affinity possibility is achieved by binding free energy calculations, which rely on the thermodynamically relevant parameters linked with the protein-ligand interactions [36,37]. The individual terms contributing to the total binding free energy and the free energy trajectories throughout the simulation were shown in Table 2 and Fig. 4 respectively. The contributions of van der Waal energy and the electrostatic energy were considerably higher than others to the binding free energy. Moreover, the SASA energy cooperated with a good addition, while the contribution of polar solvation energy was not favorable to the binding free energy.

4. Comparison with earlier reported *in-silico* analyses on SARS-CoV-2 RdRp-RNA protein

To categorize potent inhibitors against the RdRp-RNA complex of SARS-CoV-2, we compared our selected turmeric-derived compounds with the antiviral medicines Favipiravir and Remdesivir. The interacting residues and the binding free energies of Favipiravir and Remdesivir were analyzed in our previous study [31]. On comparing the results, curcumin and diacetylcurcumin showed good interactions with important residues of the NTP entry channel and catalytic center of RdRp than antiviral medicines Favipiravir and Remdesivir. Moreover, we also compared binding free energies of selected compounds with Favipiravir and Remdesivir (Table S1). Both the turmeric-derived molecules showed better binding free energies than Favipiravir and Remdesivir [31]. In addition, we also compared our results with some other computational analyses suggesting potential molecules against the RdRp of SARS-CoV-2 [38–41]. The comparison of our study with previous literature pointed out that our selected compounds (curcumin and diacetylcurcumin) had better affinity against RdRp-RNA of SARS-CoV-2 and were firmly bound to it throughout the simulation period. The strong interactions between turmeric-derived compounds and active site of RdRp compared to Remdesivir and Favipiravir also showed their potential to be developed as RdRp-RNA inhibitors. These outcomes require further validation by *in-vivo* and *in-vitro* studies.

5. Conclusion

RdRp-RNA is a promising target for developing novel SARS-CoV-2 inhibitors. In this analysis, we selected a set of six compounds from turmeric to examine their interaction poses inside the active site of the RdRp-RNA complex of SARS-CoV-2. The curcumin and diacetylcurcumin adhered firmly to the essential amino acids present in the NTP entry channel and the catalytic center required for RNA recognition and viral replication. Curcumin and diacetylcurcumin also presented the most promising binding free energies during the evaluation of MM-PBSA results. We also compared these results with the binding potential of Favipiravir and Remdesivir. The comparative analysis suggested that these compounds showed more promising potential than antiviral medicines Favipiravir and Remdesivir. Thus, the present findings revealed the efficacy of curcumin and diacetylcurcumin against the RdRp-RNA complex of SARS-CoV-2. Additionally, these *in-silico* findings require further experimental validation to advance in the drug discovery pipeline.

Declaration of competing interest

The authors declare that they have no known competing financial interests or personal relationships that could have appeared to influence the work reported in this paper.

Acknowledgment

This work was supported by The Himalayan Centre for High-throughput Computational Biology (HiCHiCoB), a BIC supported by DBT, Govt. of India. We are also grateful to CSIR-Institute of Himalayan Bioresource Technology, Palampur for providing the facilities in the form of project (MLP0201) to carry out this work. This manuscript represents CSIR-IHBT Communication No. PPME/2021/102.

Appendix A. Supplementary data

Supplementary data to this article can be found online at https://doi.org/10.1016/j.compbiomed.2021.104965.

References

[1] J.F.W. Chan, S. Yuan, K.H. Kok, K.K.W. To, H. Chu, J. Yang, F. Xing, J. Liu, C.C. Y. Yip, R.W.S. Poon, H.W. Tsoi, S.K.F. Lo, K.H. Chan, V.K.M. Poon, W.M. Chan, J. D. Ip, J.P. Cai, V.C.C. Cheng, H. Chen, C.K.M. Hui, K.Y. Yuen, A familial cluster of pneumonia associated with the 2019 novel coronavirus indicating person-to-person transmission: a study of a family cluster, Lancet 395 (2020) 514–523, https://doi.org/10.1016/S0140-6736(20)30154-9.

[2] N. Chen, M. Zhou, X. Dong, J. Qu, F. Gong, Y. Han, Y. Qiu, J. Wang, Y. Liu, Y. Wei, J. Xia, T. Yu, X. Zhang, L. Zhang, Epidemiological and clinical characteristics of 99 cases of 2019 novel coronavirus pneumonia in Wuhan, China: a descriptive study, Lancet 395 (2020) 507–513, https://doi.org/10.1016/S0140-6736(20)30211-7.

[3] C.J. Gordon, E.P. Tchesnokov, E. Woolner, J.K. Perry, J.Y. Feng, D.P. Porter, M. Götte, Remdesivir is a direct-acting antiviral that inhibits RNA-dependent RNA polymerase from severe acute respiratory syndrome coronavirus 2 with high potency, J. Biol. Chem. 295 (2020) 6785–6797, https://doi.org/10.1074/jbc.RA120.013679.

[4] W. Yin, C. Mao, X. Luan, D.D. Shen, Q. Shen, H. Su, X. Wang, F. Zhou, W. Zhao, M. Gao, S. Chang, Y.C. Xie, G. Tian, H.W. Jiang, S.C. Tao, J. Shen, Y. Jiang, H. Jiang, Y. Xu, S. Zhang, Y. Zhang, H.E. Xu, Structural basis for inhibition of the RNA-dependent RNA polymerase from SARS-CoV-2 by remdesivir, Science 368 (2020) 1499–1504, https://doi.org/10.1126/science.abc1560 (80-.).

[5] L. Subissi, C.C. Posthuma, A. Collet, J.C. Zevenhoven-Dobbe, A.E. Gorbalenya, E. Decroly, E.J. Snijder, B. Canard, I. Imbert, One severe acute respiratory syndrome coronavirus protein complex integrates processive RNA polymerase and exonuclease activities, Proc. Natl. Acad. Sci. U.S.A. 111 (2014) E3900–E3909, https://doi.org/10.1073/pnas.1323705111.

[6] S.M. Mcdonald, RNA synthetic mechanisms employed by diverse families of RNA viruses, Wiley Interdiscip. Rev. RNA. 4 (2013) 351–367, https://doi.org/10.1002/wrna.1164.

[7] K.C. Lehmann, A. Gulyaeva, J.C. Zevenhoven-Dobbe, G.M.C. Janssen, M. Ruben, H. S. Overkleeft, P.A. Van Veelen, D.V. Samborskiy, A.A. Kravchenko, A. M. Leontovich, I.A. Sidorov, E.J. Snijder, C.C. Posthuma, A.E. Gorbalenya, Discovery of an essential nucleotidylating activity associated with a newly delineated conserved domain in the RNA polymerase-containing protein of all nidoviruses, Nucleic Acids Res. 43 (2015) 8416–8434, https://doi.org/10.1093/nar/gkv838.

[8] R.N. Kirchdoerfer, A.B. Ward, Structure of the SARS-CoV nsp12 polymerase bound to nsp7 and nsp8 co-factors, Nat. Commun. 10 (2019), https://doi.org/10.1038/s41467-019-10280-3.

[9] P. Gong, O.B. Peersen, Structural basis for active site closure by the poliovirus RNA-dependent RNA polymerase, Proc. Natl. Acad. Sci. U.S.A. 107 (2010) 22505–22510, https://doi.org/10.1073/pnas.1007626107.

[10] A. Shannon, N.T.T. Le, B. Selisko, C. Eydoux, K. Alvarez, J.C. Guillemot, E. Decroly, O. Peersen, F. Ferron, B. Canard, Remdesivir and SARS-CoV-2: structural requirements at both nsp12 RdRp and nsp14 Exonuclease active-sites, Antivir. Res. 178 (2020), https://doi.org/10.1016/j.antiviral.2020.104793.

[11] M. Wang, R. Cao, L. Zhang, X. Yang, J. Liu, M. Xu, Z. Shi, Z. Hu, W. Zhong, G. Xiao, Remdesivir and chloroquine effectively inhibit the recently emerged novel coronavirus (2019-nCoV) in vitro, Cell Res. 30 (2020) 269–271, https://doi.org/10.1038/s41422-020-0282-0.

[12] M.L. Holshue, C. DeBolt, S. Lindquist, K.H. Lofy, J. Wiesman, H. Bruce, C. Spitters, K. Ericson, S. Wilkerson, A. Tural, G. Diaz, A. Cohn, L. Fox, A. Patel, S.I. Gerber, L. Kim, S. Tong, X. Lu, S. Lindstrom, M.A. Pallansch, W.C. Weldon, H.M. Biggs, T. M. Uyeki, S.K. Pillai, First case of 2019 novel coronavirus in the United States, N, Engl. J. Med. 382 (2020) 929–936, https://doi.org/10.1056/nejmoa2001191.

[13] S. Zorofchian Moghadamtousi, H. Abdul Kadir, P. Hassandarvish, H. Tajik, S. Abubakar, K. Zandi, A review on antibacterial, antiviral, and antifungal activity of curcumin, BioMed Res. Int. 2014 (2014), https://doi.org/10.1155/2014/186864.

[14] B.C. Mounce, T. Cesaro, L. Carrau, T. Vallet, M. Vignuzzi, Curcumin inhibits Zika and chikungunya virus infection by inhibiting cell binding, Antivir. Res. 142 (2017) 148–157, https://doi.org/10.1016/j.antiviral.2017.03.014.

[15] A. Niranjan, S. Singh, M. Dhiman, S.K. Tewari, Biochemical composition of curcuma longa L. Accessions, Anal. Lett. 46 (2013) 1069–1083, https://doi.org/10.1080/00032719.2012.751541.

[16] K.I. Priyadarsini, The chemistry of curcumin: from extraction to therapeutic agent, Molecules 19 (2014) 20091–20112, https://doi.org/10.3390/molecules191220091.

[17] J. Zheng, M.J. Frisch, Efficient geometry minimization and transition structure optimization using interpolated potential energy surfaces and iteratively updated hessians, J. Chem. Theor. Comput. 13 (2017) 6424–6432, https://doi.org/10.1021/acs.jctc.7b00719.

[18] D. Studio, Dassault systemes BIOVIA, discovery studio modelling environment, release 4.5, Accelrys Softw. Inc. (2015) 98–104.

[19] K. Vanommeslaeghe, E. Hatcher, C. Acharya, S. Kundu, S. Zhong, J. Shim, E. Darian, O. Guvench, P. Lopes, I. Vorobyov, A.D. Mackerell, CHARMM general force field: a force field for drug-like molecules compatible with the CHARMM all-atom additive biological force fields, J. Comput. Chem. 31 (2010) 671–690, https://doi.org/10.1002/jcc.21367.

[20] D. Van Der Spoel, E. Lindahl, B. Hess, G. Groenhof, A.E. Mark, H.J.C. Berendsen, GROMACS: fast, flexible, and free, J. Comput. Chem. 26 (2005) 1701–1718, https://doi.org/10.1002/jcc.20291.

[21] M. Parrinello, A. Rahman, Polymorphic transitions in single crystals: a new molecular dynamics method, J. Appl. Phys. 52 (1981) 7182–7190, https://doi.org/10.1063/1.328693.

[22] B. Hess, H. Bekker, H.J.C. Berendsen, J.G.E.M. Fraaije, LINCS: a linear constraint solver for molecular simulations, J. Comput. Chem. 18 (1997) 1463–1472, https://doi.org/10.1002/(SICI)1096-987X(199709)18:12<1463::AID-JCC4>3.0.CO;2-H.

[23] T. Darden, D. York, L. Pedersen, Particle mesh Ewald: an N·log(N) method for Ewald sums in large systems, J. Chem. Phys. 98 (1993) 10089–10092, https://doi.org/10.1063/1.464397.

[24] R. Kumari, R. Kumar, A. Lynn, G-mmpbsa -A GROMACS tool for high-throughput MM-PBSA calculations, J. Chem. Inf. Model. 54 (2014) 1951–1962, https://doi.org/10.1021/ci500020m.

[25] B.A.C. Rattis, S.G. Ramos, M.R.N. Celes, Curcumin as a potential treatment for COVID-19, Front. Pharmacol. 12 (2021) 1068, https://doi.org/10.3389/fphar.2021.675287.

[26] K. Rajagopal, P. Varakumar, A. Baliwada, G. Byran, Activity of phytochemical constituents of Curcuma longa (turmeric) and Andrographis paniculata against coronavirus (COVID-19): an in silico approach, Futur. J. Pharm. Sci. 6 (2020) 1–10, https://doi.org/10.1186/s43094-020-00126-x.

[27] V. Umashankar, S.H. Deshpande, H.V. Hegde, I. Singh, D. Chattopadhyay, Phytochemical moieties from Indian traditional medicine for targeting dual hotspots on SARS-CoV-2 spike protein: an integrative in-silico approach, Front. Med. 8 (2021), 672629, https://doi.org/10.3389/fmed.2021.672629.

[28] R. Singh, V.K. Bhardwaj, J. Sharma, D. Kumar, R. Purohit, Identification of potential plant bioactive as SARS-CoV-2 Spike protein and human ACE2 fusion inhibitors, Comput. Biol. Med. 136 (2021), 104631, https://doi.org/10.1016/J.COMPBIOMED.2021.104631.

[29] H.S. Hillen, G. Kokic, L. Farnung, C. Dienemann, D. Tegunov, P. Cramer, Structure of replicating SARS-CoV-2 polymerase, Nature 584 (2020) 154–156, https://doi.org/10.1038/s41586-020-2368-8.

[30] Y. Gao, L. Yan, Y. Huang, F. Liu, Y. Zhao, L. Cao, T. Wang, Q. Sun, Z. Ming, L. Zhang, J. Ge, L. Zheng, Y. Zhang, H. Wang, Y. Zhu, C. Zhu, T. Hu, T. Hua, B. Zhang, X. Yang, J. Li, H. Yang, Z. Liu, W. Xu, L.W. Guddat, Q. Wang, Z. Lou, Z. Rao, Structure of the RNA-dependent RNA polymerase from COVID-19 virus, Science 368 (2020) 779–782, https://doi.org/10.1126/science.abb7498 (80-.).

[31] V.K. Bhardwaj, R. Singh, J. Sharma, V. Rajendran, R. Purohit, S. Kumar, Bioactive molecules of Tea as potential inhibitors for RNA-dependent RNA polymerase of SARS-CoV-2, Front. Med. 8 (2021) 645, https://doi.org/10.3389/FMED.2021.684020.

[32] S. Kumar, V. Kumar Bhardwaj, R. Singh, R. Purohit, Explicit-solvent molecular dynamics simulations revealed conformational regain and aggregation inhibition of I113T SOD1 by Himalayan bioactive molecules, J. Mol. Liq. (2021), 116798, https://doi.org/10.1016/j.molliq.2021.116798.

[33] V.K. Bhardwaj, R. Singh, P. Das, R. Purohit, Evaluation of acridinedione analogs as potential SARS-CoV-2 main protease inhibitors and their comparison with repurposed anti-viral drugs, Comput. Biol. Med. 128 (2021), 104117, https://doi.org/10.1016/j.compbiomed.2020.104117.

[34] R. Singh, V.K. Bhardwaj, P. Das, R. Purohit, A computational approach for rational discovery of inhibitors for non-structural protein 1 of SARS-CoV-2, Comput, Biol. Med. (2021), 104555, https://doi.org/10.1016/j.compbiomed.2021.104555.

[35] J. Sharma, V. Kumar Bhardwaj, R. Singh, V. Rajendran, R. Purohit, S. Kumar, An in-silico evaluation of different bioactive molecules of Tea for their inhibition potency against non structural protein-15 of SARS-CoV-2, Food Chem. (2020), 128933, https://doi.org/10.1016/j.foodchem.2020.128933.

[36] R. Singh, V.K. Bhardwaj, J. Sharma, R. Purohit, S. Kumar, In-silico evaluation of bioactive compounds from tea as potential SARS-CoV-2 nonstructural protein 16 inhibitors, J. Tradit. Complement. Med (2021), https://doi.org/10.1016/j.jtcme.2021.05.005.

[37] V.K. Bhardwaj, R. Singh, J. Sharma, V. Rajendran, R. Purohit, S. Kumar, Identification of bioactive molecules from tea plant as SARS-CoV-2 main protease inhibitors, J. Biomol. Struct. Dyn. (2020) 1–10, https://doi.org/10.1080/07391102.2020.1766572.

[38] S. Koulgi, V. Jani, V.N. Mallikarjunachari Uppuladinne, U. Sonavane, R. Joshi, Natural plant products as potential inhibitors of RNA dependent RNA polymerase of Severe Acute Respiratory Syndrome Coronavirus-2, PLoS One 16 (2021), e0251801, https://doi.org/10.1371/journal.pone.0251801.

[39] M. Hosseini, W. Chen, D. Xiao, C. Wang, Computational molecular docking and virtual screening revealed promising SARS-CoV-2 drugs, Precis, Clin. Med. 4 (2021) 1–16, https://doi.org/10.1093/pcmedi/pbab001.
[40] K.S. Ebrahimi, M. Ansari, M.S. Hosseyni Moghaddam, Z. Ebrahimi, Z. salehi, M. Shahlaei, S. Moradi, In silico investigation on the inhibitory effect of fungal secondary metabolites on RNA dependent RNA polymerase of SARS-CoV-II: a docking and molecular dynamic simulation study, Comput. Biol. Med. 135 (2021), 104613, https://doi.org/10.1016/J.COMPBIOMED.2021.104613.
[41] S. Skariyachan, D. Gopal, A.G. Muddebihalkar, A. Uttarkar, V. Niranjan, Structural insights on the interaction potential of natural leads against major protein targets of SARS-CoV-2: molecular modelling, docking and dynamic simulation studies, Comput. Biol. Med. 132 (2021), 104325, https://doi.org/10.1016/J.COMPBIOMED.2021.104325.